

# Symbolic Quantile Regression for the Interpretable Prediction of Conditional Quantiles

Anonymous authors

Paper under double-blind review

## Abstract

Symbolic Regression (SR) is a well-established framework for generating interpretable or white-box predictive models. Although SR has been successfully applied to create interpretable estimates of the average of the outcome, it is currently not well understood how it can be used to estimate the relationship between variables at other points in the distribution of the target variable. Such estimates of e.g. the median or an extreme value provide a fuller picture of how predictive variables affect the outcome and are necessary in high-stakes, safety-critical application domains. This study introduces Symbolic Quantile Regression (SQR), an approach to predict conditional quantiles with SR. In an extensive evaluation, we find that SQR outperforms transparent models and performs comparably to a strong black-box baseline without compromising transparency. We also show how SQR can be used to explain differences in the target distribution by comparing models that predict extreme and central outcomes in an airline fuel usage case study. We conclude that SQR is suitable for predicting conditional quantiles and understanding interesting feature influences at varying quantiles.

## 1 Introduction

Symbolic regression (SR) offers an approach to uncover mathematical expressions that explain patterns in data. It captures these patterns in interpretable, closed-form expressions that can then be analyzed and interpreted. First, this is useful in the so-called discovery settings, where the study of the identified patterns increases the *understanding* of some phenomenon, as is the case in empirical science. Second, this is useful when making *predictions* in high-stakes domains, where accountability and safety are key considerations to use the use of predictions in decision making (Bellemare et al., 2023). In general, SR has proven to be suitable for use cases that require understanding, mitigation of risks, and keeping in mind the broader goals of making predictions. It has therefore been applied in a wide range of fields, including astrophysics (Lemos et al., 2023), economics (Verstyuk & Douglas, 2022), medicine (Virgolin et al., 2020), mechanical engineering (Kronberger et al., 2018), chemistry (Hernandez et al., 2019), and others (Märtens & Izzo, 2022; Matsubara et al., 2022), as a result.

Quantile regression (QR), on the other hand, focuses on making predictions at different locations of the outcome distribution by estimating different conditional quantile functions as visualized in Figure 1. Unlike traditional regression, which focuses on predicting a single central location of the outcome variable, QR accounts for variability and extremes, offering more robust predictions that can be used for better decision making. This is of paramount importance

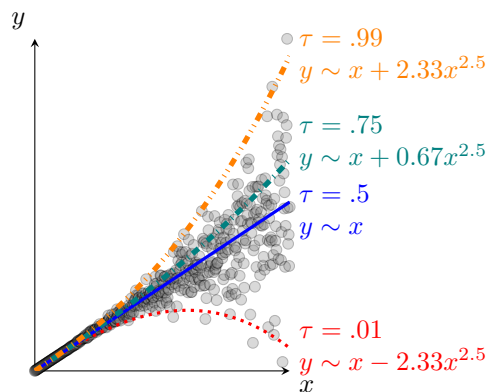


Figure 1: Conditional quantile functions at various quantile levels  $\tau$  for a distribution where the variance of the target  $y$  changes with the level of the independent variable  $x$ .

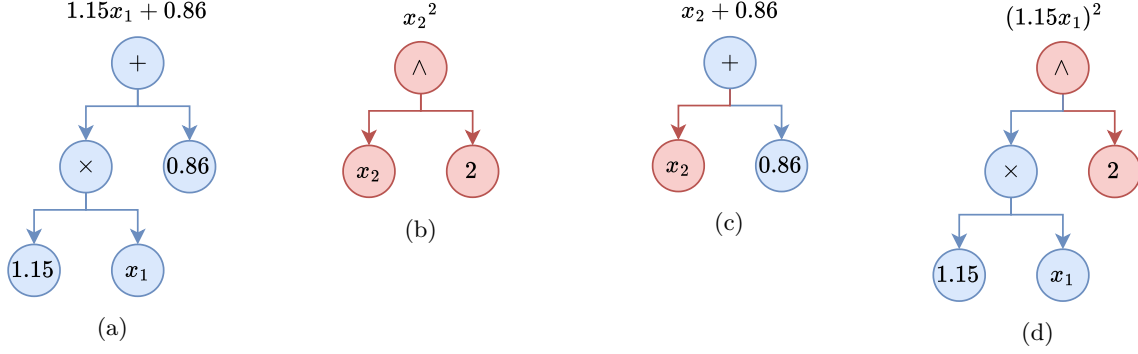


Figure 2: Two symbolic expressions are represented as trees (2a and 2b), and combined through *crossover* to form two new expressions (2c and 2d).

in contexts where data exhibit heteroskedasticity, such as in economics (Buchinsky, 1995), or when it is necessary to ensure that a certain proportion, say 90%, of actual values is lower than the predicted values, such as in survival analysis, reliability engineering, and healthcare (Hu et al., 2020; Koenker & Geling, 2001; Zheng et al., 2022).

However, current state-of-the-art QR models are black boxes and lack the interpretability required for high-stakes decision making that SR offers by design. This study therefore proposes a novel combination of SR and QR that provides interpretable predictive models for a given quantile level. Symbolic Quantile Regression (SQR) jointly optimizes for predictive performance and interpretability of the generated expressions by minimizing an established QR loss known as the pinball loss together with a loss for the interpretability of the expression.

We compare SQR with a number of state-of-the-art QR approaches in different quantiles in a substantial benchmark of 122 regression data sets. We assess its predictive performance and interpretability and find that SQR finds interpretable models while maintaining a predictive performance comparable to or better than state-of-the-art black-box models. We also present a case study from the commercial aviation domain, in which we apply SQR to a fuel consumption prediction problem to explore why some flights consume more fuel with the goal of reducing CO2 emissions. By comparing expressions that describe central and extreme fuel consumption levels, we find that higher velocities resulting from later departures explain extreme fuel usage. We thereby not only show that SQR is competitive in its predictive performance but also showcase how it can be used to create actionable insights on a real-world problem. Hence, SQR addresses key challenges related to the safe adoption of machine learning techniques in safety-critical and high-stakes domains by providing interpretable estimates of conditional quantile functions.

## 2 Background and Related Work

### 2.1 Symbolic Regression

Symbolic regression (SR) can be defined as a search process over the space of concise, closed-form mathematical expressions for an expression that best fits a dataset, thereby revealing the underlying patterns. For an i.i.d. data set  $D := (\mathbf{X}, \mathbf{y})$ , where each input  $\mathbf{X}_{i,:} \in \mathbb{R}^d$  and output  $\mathbf{y}_i \in \mathbb{R}$ , the goal of SR is to find a function  $f: \mathbb{R}^d \rightarrow \mathbb{R}$  that accurately predicts the output given the input. In SR, the function  $f$  represents a mathematical expression that captures the relationship between explanatory and target variables, and takes the form  $f(\mathbf{X}_{i,:}) = \mathbf{y}_i + \epsilon$  for an error term  $\epsilon$  (Koza, 1994).

The expression  $f$  is modeled as a sequence of *tokens*, which include mathematical operations such as addition (+), subtraction (−), trigonometric functions ( $\sin()$ ), input features ( $\mathbf{X}_{:,1} \dots \mathbf{X}_{:,d}$ ) and constants in  $\mathbb{R}$ . The search process aims to minimize a loss function, which is typically a measure of predictive performance, such as the mean squared error for regression tasks or the F1 score for binary classification, along with some measure of the interpretability of the expression (Visbeek et al., 2024). The interpretability of the

Table 1: Complexity scores for operators.

Token	Complexity
$+$ , $-$ , $\times$ , feature, constant	1
$\div$ , square	2
$\sin$ , $\cos$	3
$\exp$ , $\log$ , $\sqrt{\cdot}$	4

expression is typically defined as its parsimony, i.e. the sum of the complexity scores assigned to each token, as illustrated in Table 1.

Historically, SR has been tackled using genetic programming (Koza, 1994), see Figure 2. Genetic programming is inspired by evolutionary biology and mimics natural selection through operations like crossover and mutation to evolve candidate solutions over generations. By iteratively combining and modifying instances in a population of solutions, it adheres to the principle of “survival of the fittest” by selecting models based on their performance according to a predefined loss or fitness function. The flexibility and robustness of population-based evolutionary methods make it a powerful tool for exploring the combinatorial solution space of mathematical expressions in SR.

Discovering an expression that is both predictive and interpretable not only enhances understanding of the phenomena underlying the data (the *discovery* use case) but also provides a reliable means for predicting the target variable (the *prediction* use case). In recent years, several extensions of the SR framework have emerged, including integrations with deep reinforcement learning and adaptations for classification tasks (Landajuela et al., 2022; Visbeek et al., 2024). Furthermore, the field of SR has been further developed through the introduction of various data sets and software tools that have advanced the research and practical applicability of SR (Orzechowski et al., 2018; Cranmer et al., 2020; La Cava et al., 2021).

## 2.2 Interpretability

Interpretability in machine learning has traditionally been evaluated using sparsity or simplicity metrics within a given model class (Jo et al., 2023). For instance, in linear models, interpretability is often measured by counting the number of nonzero coefficients, while in decision trees, interpretability is typically assessed by the number of nodes (i.e., branches and leaves). However, these metrics are limited because they do not allow meaningful comparisons across different model classes, as each class defines sparsity differently.

To address this limitation, the concept of decision complexity has been introduced as a more generalizable metric for sparsity that can be applied across various model classes. Decision complexity is defined as “the minimum number of parameters required for a classifier to make a prediction on a new data point” (Jo et al., 2023). This notion is generally referred to as parsimony in recent work and standardizes the measurement of interpretability by focusing on the essential components needed for decision making, regardless of the model type.

## 3 Symbolic Quantile Regression

We now turn to the main technical contribution, which is the extension of SR so that it can be used to predict various locations of the target distributions while maintaining interpretability. We formalize this problem as follows. Let  $(\mathcal{X}, \mathcal{Y})$  be random variables where  $\mathcal{X} \in \mathbb{R}^d$  represents a  $d$  dimensional input and  $\mathcal{Y} \in \mathbb{R}$  the response variable or target. Our goal is to estimate the conditional quantile function  $Q_{\mathcal{Y}}(\tau|\mathcal{X} = X)$  for a specified quantile level  $\tau \in (0, 1)$ :

$$Q_{\mathcal{Y}}(\tau|\mathcal{X} = X) := \inf \{q \in \mathbb{R} : \mathbb{P}(\mathcal{Y} \leq q|\mathcal{X} = X) \geq \tau\}. \quad (1)$$

We assume the presence of a data set of i.i.d. samples  $D := (\mathbf{X}, \mathbf{y})$  of size  $n$  where  $(\mathbf{X}_{i,:}, \mathbf{y}_i)_{i=0}^n \sim (\mathcal{X}, \mathcal{Y})$ .

### 3.1 Estimating Conditional Quantiles

A common approach to estimating the conditional quantile function  $Q_Y(\tau|\mathcal{X})$  given a dataset is to use empirical risk minimization with the use of the pinball loss. This loss function resembles an asymmetric absolute value function and penalizes underestimation and overestimation differently, making it well-suited for quantile estimation tasks where such asymmetries are meaningful. Specifically, for a given error  $\varepsilon_i := y_i - f(X_i)$  where  $f(X_i)$  is the predicted value, the pinball loss is defined as:

$$L_\tau(\varepsilon_i) = \begin{cases} (\tau - 1)(\varepsilon_i) & \text{if } \varepsilon_i \geq 0, \\ \tau(\varepsilon_i) & \text{if } \varepsilon_i < 0 \end{cases} \quad (2)$$

Figure 3 visualizes this function for different quantile levels  $\tau$ . For example, with  $\tau = .9$ , an underestimate  $\varepsilon = -1$  is penalized nine times more than its corresponding overestimate  $\varepsilon = 1$ . As a result, the optimization is biased toward over-prediction, yielding estimates that align with the 90th empirical conditional quantile.

SQR estimates the conditional quantiles of a distribution  $P$  with empirical risk minimization. Let  $P$  be a distribution in  $\mathbb{X} \times \mathbb{R}$ , with  $\mathbb{X}$  being an arbitrary set equipped with a  $\sigma$  parameter. Here,  $\mathbb{R}$  represents the target space and  $\mathbb{X}$  the input feature space. That is, each  $\mathbf{x} \in \mathbb{X}$  corresponds to a set of predictor variables and each  $\mathbf{y} \in \mathbb{R}$  corresponds to an observed response variable. The conditional quantile function  $F_{\tau,P}^*(\mathbf{x})$  for  $\mathbf{x} \in \mathbb{X}$  is defined as:

$$F_{\tau,P}^*(\mathbf{x}) := \left\{ t \in \mathbb{R} : P((-\infty, t] | \mathbf{x}) \geq \tau \text{ and } P([t, \infty) | \mathbf{x}) \geq 1 - \tau \right\} \quad (3)$$

This function identifies the threshold  $t$  such that the probability of observing a value below  $t$  (given  $\mathbf{x}$ ) is at least  $\tau$ , and the probability of observing a value above this threshold is at least  $1 - \tau$ . The associated expected risk  $R$  for a predictor  $f : \mathbb{X} \rightarrow \mathbb{R}$  is:

$$\begin{aligned} R_{L,P}(f) &= \mathbb{E}_{(\mathbf{X}, \mathbf{y}) \sim P} [L_\tau(\mathbf{y}, f(\mathbf{X}))] \\ &= \int_{\mathbb{X} \times \mathbb{R}} L_\tau(\mathbf{y}, f(\mathbf{X})) dP(\mathbf{X}, \mathbf{y}) \end{aligned} \quad (4)$$

and the objective is to find  $f_{\tau,P}^*$  that minimizes this risk to effectively balance underestimation and overestimation for the desired quantile level.

However, while empirical risk minimization provides a principled means to estimate quantiles from data, it is fundamentally based on the quality and representativeness of the observed sample. As evident in Equation 4, minimizing the empirical risk does not guarantee that the resulting model perfectly captures the true conditional quantile. This issue is particularly pronounced in regions of the distribution where data is sparse or noisy, such as the tails, which are often the focus in high-stakes settings.

Crucially, this challenge is not unique to SQR or the use of pinball loss. Rather, this is a fundamental limitation that arises in any approach to quantile estimation from finite data. As such, careful evaluation and validation are essential to ensure robust quantile estimation, and our experiments are designed with these considerations in mind.

### 3.2 Optimizing for Interpretability

Having established a suitable loss for estimating the conditional quantile function, we now turn to the objective of interpretability. We operationalize interpretability as *parsimony*, defined as a preference for concise

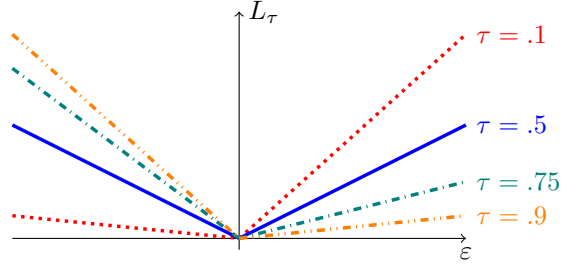


Figure 3: Pinball loss function for various values of conditional quantile  $\tau$ . Errors  $\varepsilon$  are penalized asymmetrically for  $\tau \neq 0.5$  to predict values close to the desired  $\tau$ .

symbolic expressions with minimal structural and functional complexity. Parsimony is particularly suitable in high stakes settings, where trust and safety are paramount, as simpler models are more amenable to human inspection, validation, and understanding, thus promoting trust and perceived trustworthiness (Bansal et al., 2019).

We define parsimony following established conventions (Petersen et al., 2021; 2020) For an expression  $f$ , composed of tokens  $t$  with associated token complexity scores  $|t|$ , as detailed in Table 1, its parsimony  $|f|$  is defined as:

$$|f| = \sum_{t \in f} |t|. \quad (5)$$

Since we may not know what level of interpretability is necessary and attainable, we construct a Pareto front (PF) of the best expressions across a range of parsimony levels, from which a single expression with optimal predictive performance and acceptable interpretability can be selected. A preferred solution can then be selected from this front based on, e.g., the elbow method or on requirements from the use case or domain at hand (Thorndike, 1953).

Formally, the optimization problem for SQR is therefore:

$$\text{PF}_\tau(\mathbb{C}, D) = \left\{ \arg \min_{f \in \mathcal{F}} \left( \sum_{i=1}^n L_\tau(\varepsilon_i) \right) \mid |f| = c, c \in \mathbb{C} \right\} \quad (6)$$

where  $\mathcal{F}$  denotes the space of all possible expressions that can be constructed from the token library and  $\mathbb{C} \subset \mathbb{N}$  a set of possible parsimony scores under consideration.

### 3.3 Optimization

To perform symbolic quantile regression, we build on PySR, a symbolic regression optimization engine that combines evolutionary search with local optimization and adaptive regularization by Cranmer (2023). We use this engine due to its support for these features, its strong empirical performance in noisy conditions, and ease in implementation of research prototypes.

The core algorithm maintains multiple evolving populations of symbolic expressions across parallel compute threads. The multi-population architecture promotes diversity and robustness by preventing the global search process from collapsing prematurely onto narrow regions of the solution space. Each population undergoes repeated cycles of evolution, simplification, and optimization as visualized in Figure 4. During evolution, expressions are modified via mutation and crossover operators to explore new structural forms. The simplification step consists of algebraic rewriting to reduce redundancy and improve interpretability. To fine-tune numerical parameters, the scalar constants within the expressions are optimized locally with BFGS (Nocedal & Wright, 2006).

To regulate selection pressure and prevent premature convergence, the algorithm introduces age-based regularization and simulated annealing. Rather than eliminating the least fit individuals, age-regularization favors younger individuals to promote exploration and maintain diversity by ensuring that newly generated expressions are continually integrated into the population Real et al. (2019). Simulated annealing further helps balance exploration and exploitation by probabilistically accepting weaker candidates early in the search.

In line with our overall objective, the problem is framed as a multi-objective optimization problem balancing predictive performance and parsimony. During optimization, an adaptive parsimony penalty is incorporated into the fitness function to ensure diversity of complexity levels within the population. This penalty is based on a heuristic quantifying how frequently and recently expressions of a given complexity appear as follows. Overrepresented complexity levels are temporarily penalized to encourage the search to visit underrepresented regions, which are associated with simpler or more complex solutions.

After optimization concludes, a Pareto front of non-dominated solutions is constructed, explicitly avoiding the need to combine accuracy and parsimony into a single scalar objective. The final model is selected directly from this Pareto front using e.g. the elbow method.

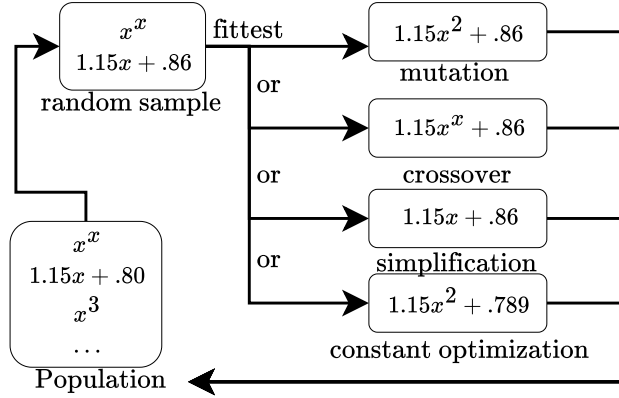


Figure 4: Evolutionary optimization process (from Cranmer (2023)).

This combination of evolutionary search, local refinement, age-aware diversity mechanisms, and adaptive complexity control allows symbolic regression to remain effective under high noise, making it well suited for modeling quantile functions where interpretability and robustness are critical.

## 4 Experiments

We evaluate SQR empirically on a substantive benchmark consisting of 122 datasets of varying dimensionality, and compare it to existing black-box and transparent models for QR. We focus on the predictions in a central and extreme location of the target variable with  $\tau = .5, \tau = .9$ , respectively, to assess the performance in typical and extreme conditions. See the appendices for all details about the datasets, statistical testing, and additional results.

### 4.1 Datasets

SRBench (La Cava et al., 2021) is the de facto standard for evaluating SR approaches. It comprises 252 synthetic and real-world data sets with and without noise in the target variable. We exclude all data sets without noise in the target variable for our purposes, because the conditional quantiles for a target without noise all lie at the same location. The noisy condition is also more realistic. This leaves an evaluation on 122 real-world and synthetic datasets of varying dimensionality and size.

### 4.2 Baselines

A set of models with state-of-the-art predictive performance and varying degrees of interpretability and parsimony were selected. Both transparent and black-box models were included to highlight the strengths and weaknesses of each approach in the context of quantile regression.

**Linear Quantile Regressor (LQR)** by Seabold & Perktold (2010) is widely adopted for its simplicity and interpretability. LQR cannot capture nonlinearities, but it is robust to overfitting and generally considered as highly transparent.

**Quantile Decision Tree (QDT)** by Pedregosa et al. (2011) is regarded as a transparent model, but may suffer from poor performance on small datasets, may overfit and some times struggles with modeling linearities.

**LGBM Quantile Regressor (LGBM)** by Ke et al. (2017) is selected for its ability to capture complex relationships in large data sets. Since LGBM provides black-box models, it serves as a high-performance, albeit non-transparent, model.

**SQR** is our approach trained on the full training data set.

**SQR10k** is our approach trained on a random sample of at most 10k train instances. For datasets smaller than 10k, we train without sampling. We include this version of the approach to assess the effect of limited data when aiming for a model with high interpretability.

SQR was implemented and evaluated with the PySR software and default hyperparameters were used. (Cranmer et al., 2020).<sup>1</sup> The hyperparameters of LGBM, QDT, and LQR were optimized per dataset using Optuna and five-fold cross validation (Akiba et al., 2019).

### 4.3 Evaluation

We include metrics based on best practices and recommendations from the literature (Steinwart & Christmann, 2011; Chung et al., 2021), and use a combination of metrics to ensure that our evaluations are valid given the challenges of estimating conditional quantiles on finite samples.

Firstly, we employ a normalized version of the pinball loss that enables comparisons across datasets and is known as the quantile loss. This measure averages the loss in Equation 2 in all instances of the test set. This total average loss is then normalized to  $[0, 1]$  using the range of the target variable to ensure that data sets with target variables with a large range do not have an outsized influence on the evaluation:

$$\text{Normalized Quantile Loss (nql)} := \frac{\frac{1}{n} \sum_{i=1}^n L_{\tau}(\mathbf{y}_i, f(\mathbf{X}_{i,:}))}{\max(\mathbf{y}) - \min(\mathbf{y})}. \quad (7)$$

for all  $n$  items in some test set.

We complement the normalized quantile loss with a measure that expresses whether predictions align well with the specified quantile level  $\tau$ , known as the absolute coverage error:

$$\text{Absolute Coverage Error (ace)} := |\text{Cov}(\tau) - \tau| \quad (8)$$

for an empirical coverage defined as:

$$\text{Cov}(\tau, D) = \frac{1}{n} \sum_{i=1}^n \mathbf{1}(\mathbf{y}_i \leq f(\mathbf{X}_{i,:})). \quad (9)$$

For example, when  $\tau = .9$ , the empirical coverage ideally reflects a 90% proportion of the test data that falls below the predicted quantile.

Additionally, we include model parsimony as a measure to capture the notion of interpretability. Since we are interested in comparing the parsimony of various models across datasets, we opted to use average parsimony across models and datasets as defined in Equation equation 5. Finally, we report run times to assess the practical feasibility of our approach. In doing so, we note that this comparison is between a research prototype implementation for SQR, against highly optimized industry-grade implementations of the baselines.

Five-fold cross-validation was used, resulting in five different test scores for every measure for the 90th and 50th quantiles. These scores were averaged per dataset, resulting in two scores for each measure per model for every data set. We present the average (mean) and standard deviation (SD) over all data sets in this Section. Nonparametric statistical tests were used for all results due to nonnormality of the data according to the Shapiro-Wilk test ( $p < 0.05$ ) for most results. For comparisons between measures and quantiles, the Friedman test was used. Significant results were further analyzed using the Paired Wilcoxon signed rank test. Bonferroni correction was applied in all cases of multiple comparisons.

### 4.4 Results

Table 2 lists the predictive performance metrics and shows that SQR is the transparent model that performs best. The results are consistent at both quantile levels  $\tau = .5$  and  $\tau = .9$ . This table further shows that SQR achieves this strong performance at a lower cost in terms of parsimony than transparent alternatives.

<sup>1</sup><https://anonymous.4open.science/r/SQR-184C/README.md>

Table 2: Comparison across normalized quantile loss equation 7, absolute coverage error equation 8, parsimony equation 5, and transparency (last column). **Bold** indicates significant best among transparent models.

	Normalized Quantile Loss		Absolute Coverage Error		Parsimony		Transparent
	$\tau = .5$	$\tau = .9$	$\tau = .5$	$\tau = .9$	$\tau = .5$	$\tau = .9$	
LGBM	.042 $\pm$ .022	.025 $\pm$ .012	.064 $\pm$ .070	.039 $\pm$ .038	–	–	
LQR	.059 $\pm$ .030	.059 $\pm$ .044	<b>.065</b> $\pm$ .081	.287 $\pm$ .207	19.54 $\pm$ 21.14	19.57 $\pm$ 21.04	✓
QDT	.039 $\pm$ .017	.020 $\pm$ .001	.088 $\pm$ .10	.066 $\pm$ .057	323.46 $\pm$ 1306.47	210.82 $\pm$ 1080.43	✓
SQR	<b>.030</b> $\pm$ .021	<b>.015</b> $\pm$ .013	.082 $\pm$ .092	<b>.049</b> $\pm$ .061	<b>10.04</b> $\pm$ 4.09	<b>9.85</b> $\pm$ 3.67	✓
SQR10K	.033 $\pm$ .022	.017 $\pm$ .013	.084 $\pm$ .084	.058 $\pm$ .070	9.82 $\pm$ 4.40	9.71 $\pm$ 4.22	✓

Table 3: Average run time (ms).

	$\tau = .5$	$\tau = .9$
LGBM	5.01 $\pm$ 46.61	9.81 $\pm$ 94.02
LQR	10.31 $\pm$ 32.36	11.51 $\pm$ 37.87
QDT	0.32 $\pm$ 0.68	0.35 $\pm$ 0.77
SQR	3299.12 $\pm$ 11652.14	1906.94 $\pm$ 5757.59
SQR10K	166.77 $\pm$ 171.50	166.36 $\pm$ 167.87

To further evaluate the performance of interpretable models in the three selected metrics, we performed statistical significance tests to assess differences per pair (metric, quantile level) pair for all transparent models. Each test’s null hypothesis states that there are no significant differences between two models for a specific metric-quantile level pair, following this template:

- $H_{\text{null}}^{\text{metric},.5}$ : The differences in ‘metric’ between models at the  $\tau = .5$  quantile level are not significant, and model A cannot be said to significantly outperform model B or vice versa.

A two-stage analysis approach was employed to reduce the number of statistical tests. First, significant differences between results were assessed per pair of metric-quantile level. If differences were significant, we evaluated which model was the significant best.

Statistical significance at the metric-quantile level was first assessed using a Bonferroni corrected Friedman test per pair at the metric-quantile level. Given three metrics and two quantile levels, the corrected alpha level was set to  $\alpha = \frac{0.05}{6} \approx 0.00833$ . Significant differences were observed at both quantiles, for all of normalized quantile loss, absolute coverage error and parsimony.

A second stage of statistical tests was used to assess *which* of the models significantly outperform the others using pairwise comparisons in a Bonferroni-corrected Wilcoxon signed rank test. With 18 pairwise comparisons in total, the corrected alpha level was established at  $\alpha = \frac{0.05}{18} \approx 0.00278$ . The performance improvements of SQR over other transparent models were significant for all metrics and conditions, with the exception of the improvement of SQR over QDT in absolute coverage error for  $\tau = .5$ .

Considering all statistical tests together, we evaluate the hypotheses as follows. For  $\tau = .5$ :

- $H_{\text{null}}^{\text{nql},.5}$  Significant differences in normalized quantile loss were found between SQR and both LQR and QDT, with SQR performing best.
- $H_{\text{null}}^{\text{ace},.5}$  Significant differences in absolute coverage error were found between LQR and the other models, with LQR performing best.
- $H_{\text{null}}^{\text{pars},.5}$  Significant differences were found in parsimony between SQR and both LQR and QDT, with SQR showing the lowest parsimony.



Table 4: Features used for predicting and explaining airline fuel usage.

Abbreviation	Name	Description
ASF	Adjusted Speeding Factor	Speeding due to departure delays.
GCD	Great Circle Distance	Shortest distance between departure and arrival airports (km).
AWC	Average Wind Component	Average wind component relative to the aircraft’s direction.
TP	Total Pax	Total number of passengers on the flight.

For  $\tau = .9$ :

$H_{\text{null}}^{\text{ntl},.9}$  Significant differences were found in normalized quantile loss between SQR and both LQR and QDT, with SQR performing best.

$H_{\text{null}}^{\text{ace},.9}$  Significant differences for absolute coverage error were found between SQR and both LQR and QDT, with SQR performing best.

$H_{\text{null}}^{\text{pars},.9}$  Significant differences in parsimony were found between SQR and both LQR and QDT, with SQR showing the lowest complexity.

These results indicate that SQR generally outperforms the other interpretable models in both predictive performance and interpretability when trained on the full training set.

Looking at the runtime results in Table 3, we find that the prototype implementation of SQR comes at substantial additional computational cost. However, this cost can be significantly brought down through sampling as the run times for SQR10K show: these significantly bring down the run times at limited cost in predictive performance or parsimony. Furthermore, we believe that the runtime of our approach can be reduced by two orders of magnitude based on a recent comparison of the underlying optimization framework with a highly optimized implementation cited Tonda2024.

## 5 Understanding Extreme Airplane Fuel Use

We applied SQR to a real-world use case to assess its practical utility for creating interpretable predictions at different locations of the target variable. In this case study, the first objective is to predict extreme quantiles to ensure sufficient fuel is loaded. Interpretability is a prerequisite here due to industry regulations which require transparent models that are subject to human oversight. The second objective is to explain differences between central and extreme fuel usage in order to reduce fuel consumption and CO2 emissions.

To pursue the initial goal of accurate predictions, we use SQR to create expressions that capture extreme ( $\tau = .9$ ) fuel consumption across flights between two locations. To pursue the second goal of understanding differences between central and extreme fuel usage, we additionally create expressions for the central conditional quantile ( $\tau = .5$ ) function. By comparing the resulting expressions, we will gain understanding of why fuel usage may be high for some flights in comparison to others, demonstrating SQR’s potential to uncover actionable insights by predicting patterns in the data at different quantiles.

### 5.1 Dataset

The dataset for this use case contains flights of the Boeing 777 aircraft operated by an internationally operating airline company. The target variable is the amount of fuel consumed during flight in kg, all explanatory variables are listed in Table 4. The adjusted speeding factor (ASF) is a concept that captures pilot speeding behavior. It is defined based on scheduled and actual departure times and flight duration. If the plane departed earlier than scheduled and the actual flight duration is equal to or longer than the planned flight duration, then ASF is the ratio of actual to planned flight duration. If the plane departs later than scheduled and the actual flight duration is shorter than the planned duration, ASF is the ratio of planned to actual duration. In all other cases, ASF is set to 1.0, indicating no speeding adjustment. A

selection was made of flights operated on two days of the week for a duration of four years (2019-2023) to ensure a sufficient size and to combat the effects of passenger load conditions, weather conditions and airport congestion.

## 5.2 Results

We now present, analyze and compare the expressions for the 50th and 90th quantiles, and compare these in order to explain extreme airline fuel usage. We highlight how ASF, a variable capturing speeding, impacts fuel consumption differently under median and extreme conditions.

For the 50th quantile, the selected expression produces a pinball loss of 1746.29 and an empirical coverage of 0.51:

$$f_{\tau=50} = 7.216 \times GCD + 0.003 \times GCD \times (TP + 0.045 \times GCD - 7.22 \times AWC) + 1676.6 \quad (10)$$

The expression suggests a linear relationship primarily driven by the traveled distance (GCD), with interactions involving the number of passengers (TP) and wind conditions (AWC). The coverage is close to the target quantile level.

The 90th quantile expression produced a pinball loss of 944.59 and an empirical coverage of 0.91, again close to the target quantile level:

$$f_{\tau=90} = 2360.4 \times ASF^2 + \frac{GCD \times (TP + 2126.03)}{238.2 \times ASF + 0.45 \times AWC} \quad (11)$$

The expression suggests complex interactions in which the speeding component (ASF) dominates other factors such as travel distance (GCD), passenger load (TP) and wind conditions (AWC).

The expressions reveal remarkable differences in the impact of speeding (ASF) on fuel consumption. For the 50th quantile, fuel consumption is primarily driven by distance, with moderate effects from passenger load and wind conditions. In contrast, the 90th quantile shows that speeding plays a crucial role and indicates that speeding leads to extreme fuel consumption. Hence, a decrease in speeding is expected to decrease extreme fuel consumption. This insight may be used by airlines that aim to reduce fuel consumption and CO2 emissions, for instance by focusing efforts on a timely departure or a schedule with planned arrival times that accommodate for departure delays.

## 6 Discussion

We introduced Symbolic Quantile Regression (SQR), a novel method that combines Symbolic Regression (SR) with Quantile Regression (QR) to produce interpretable predictors of conditional quantiles. In an extensive benchmark, SQR demonstrated competitive accuracy at both the median (50th) and upper (90th) quantiles, outperforming related methods across predictive performance, empirical calibration, and interpretability metrics.

SQR balances predictive accuracy with model transparency, a key requirement in domains where interpretability is not just desirable but essential. Our results suggest that SQR is effective in estimating quantiles with concise symbolic models, making it particularly suitable for applications in high-stakes settings such as healthcare, finance, engineering, and scientific discovery. In these contexts, *understanding* the conditions under which certain outcomes arise is as important as the *predictions* of outcomes themselves.

A real-world case study in the airline sector further illustrated the practical utility of SQR. By modeling fuel consumption across quantiles, SQR revealed the impact of speeding on high fuel usage. This insight can inform operational strategies to reduce both costs and environmental impact. The strong empirical coverage of the model in extreme conditions and its interpretability underscore its potential for integration into daily decision-making pipelines in the high-stakes domain of commercial aviation.

Despite these promising results, several limitations merit discussion. Our use of a token-based complexity metric to operationalize interpretability, while standard and scalable across datasets, remains a proxy. Future

work should explore adaptive and human-centered interpretability functions, potentially learned in human-in-the-loop settings to better capture domain- and user-specific notions of simplicity and relevance (Nadizar et al., 2024).

Another possibility for future research lies in the extension of SQR to calibrated prediction intervals, combining it with methods such as conformal prediction (Fontana et al., 2023) or joint optimization frameworks for interval predictors (Soares & Fagundes, 2018). These directions would extend and complement SQR to further enhance the reliability of symbolic predictive models, under e.g. distributional shift or uncertainty.

In conclusion, SQR delivers accurate and interpretable quantile estimates with empirical robustness and demonstrated real-world relevance. It advances the field’s broader goals of safe, explainable and actionable AI by supporting decision-making with accurate *predictions*, and by providing an *understanding* of the underlying phenomena. With its unique combination of modeling various locations of the target distribution and the usage of symbolic functions to capture complex relationships concisely, SQR represents a compelling step in, and useful tool for, transparent and robust machine learning.

## References

- Takuya Akiba, Shotaro Sano, Toshihiko Yanase, Takeru Ohta, and Masanori Koyama. Optuna: A next-generation hyperparameter optimization framework. In *Proc. of the 25th ACM SIGKDD international conference on knowledge discovery & data mining*, pp. 2623–2631, 2019.
- Gagan Bansal, Besmira Nushi, Ece Kamar, Walter S Lasecki, Daniel S Weld, and Eric Horvitz. Beyond accuracy: The role of mental models in human-ai team performance. In *Proceedings of the AAAI conference on human computation and crowdsourcing*, volume 7, pp. 2–11, 2019.
- Marc G Bellemare, Will Dabney, and Mark Rowland. *Distributional reinforcement learning*. MIT Press, 2023.
- Moshe Buchinsky. Quantile regression, box-cox transformation model, and the us wage structure, 1963–1987. *Journal of econometrics*, 65(1):109–154, 1995.
- Youngseog Chung, Willie Neiswanger, Ian Char, and Jeff Schneider. Beyond pinball loss: Quantile methods for calibrated uncertainty quantification. *NeurIPS*, 34:10971–10984, 2021.
- Miles Cranmer. Interpretable machine learning for science with pysr and symbolicregression.jl. *arXiv preprint arXiv:2305.01582*, 2023.
- Miles Cranmer, Alvaro Sanchez Gonzalez, Peter Battaglia, Rui Xu, Kyle Cranmer, David Spergel, and Shirley Ho. Discovering symbolic models from deep learning with inductive biases. *NeurIPS*, 33:17429–17442, 2020.
- Matteo Fontana, Gianluca Zeni, and Simone Vantini. Conformal prediction: a unified review of theory and new challenges. *Bernoulli*, 29(1):1–23, 2023.
- Alberto Hernandez, Adarsh Balasubramanian, Fenglin Yuan, Simon AM Mason, and Tim Mueller. Fast, accurate, and transferable many-body interatomic potentials by symbolic regression. *NPJ Computational Materials*, 5(1):112, 2019.
- Liangyuan Hu, Lihua Li, Jiayi Ji, and Mark Sanderson. Identifying and understanding determinants of high healthcare costs for breast cancer: a quantile regression machine learning approach. *BMC health services research*, 20:1–10, 2020.
- Nathanael Jo, Sina Aghaei, Jack Benson, Andres Gomez, and Phebe Vayanos. Learning optimal fair decision trees: Trade-offs between interpretability, fairness, and accuracy. In *Proc. of the 2023 AAAI/ACM Conference on AI, Ethics, and Society*, pp. 181–192, 2023.
- Guolin Ke, Qi Meng, Thomas Finley, Taifeng Wang, Wei Chen, Weidong Ma, Qiwei Ye, and Tie-Yan Liu. Lightgbm: A highly efficient gradient boosting decision tree. *NeurIPS*, 30, 2017.

- Roger Koenker and Olga Geling. Reappraising medfly longevity: a quantile regression survival analysis. *Journal of the American Statistical Association*, 96(454):458–468, 2001.
- John R Koza. Genetic programming as a means for programming computers by natural selection. *Statistics and computing*, 4:87–112, 1994.
- Gabriel Kronberger, Michael Kommenda, Andreas Promberger, and Falk Nickel. Predicting friction system performance with symbolic regression and genetic programming with factor variables. In *Proc. of the Genetic and Evolutionary Computation Conference*, pp. 1278–1285, 2018.
- William La Cava, Bogdan Burlacu, Marco Virgolin, Michael Kommenda, Patryk Orzechowski, Fabrício Olivetti de França, Ying Jin, and Jason H Moore. Contemporary symbolic regression methods and their relative performance. *NeurIPS*, 2021, 2021.
- Mikel Landajuela, Chak Shing Lee, Jiachen Yang, Ruben Glatt, Claudio P Santiago, Ignacio Aravena, Terrell Mundhenk, Garrett Mulcahy, and Brenden K Petersen. A unified framework for deep symbolic regression. *NeurIPS*, 35:33985–33998, 2022.
- Pablo Lemos, Niall Jeffrey, Miles Cranmer, Shirley Ho, and Peter Battaglia. Rediscovering orbital mechanics with machine learning. *Machine Learning: Science and Technology*, 4(4):045002, 2023.
- Marcus Mörtens and Dario Izzo. Symbolic regression for space applications: Differentiable cartesian genetic programming powered by multi-objective memetic algorithms. *arXiv preprint arXiv:2206.06213*, 2022.
- Yoshitomo Matsubara, Naoya Chiba, Ryo Igarashi, and Yoshitaka Ushiku. Rethinking symbolic regression datasets and benchmarks for scientific discovery. *arXiv preprint arXiv:2206.10540*, 2022.
- Giorgia Nadizar, Luigi Rovito, Andrea De Lorenzo, Eric Medvet, and Marco Virgolin. An analysis of the ingredients for learning interpretable symbolic regression models with human-in-the-loop and genetic programming. *ACM Transactions on Evolutionary Learning and Optimization*, 4(1):1–30, 2024.
- Jorge Nocedal and Stephen J Wright. *Numerical optimization*. Springer, 2006.
- Patryk Orzechowski, William La Cava, and Jason H Moore. Where are we now? a large benchmark study of recent symbolic regression methods. In *Proc. of the genetic and evolutionary computation conference*, pp. 1183–1190, 2018.
- Fabian Pedregosa, Gaël Varoquaux, Alexandre Gramfort, Vincent Michel, Bertrand Thirion, Olivier Grisel, Mathieu Blondel, Peter Prettenhofer, Ron Weiss, Vincent Dubourg, et al. Scikit-learn: Machine learning in python. *JMLR*, 12(Oct):2825–2830, 2011.
- Brenden K Petersen, Mikel Landajuela Larma, Terrell N Mundhenk, Claudio Prata Santiago, Soo Kyung Kim, and Joanne Taery Kim. Deep symbolic regression: Recovering mathematical expressions from data via risk-seeking policy gradients. In *Proc. of ICLR*, 2020.
- Brenden K Petersen, Mikel Landajuela Larma, Terrell N. Mundhenk, Claudio Prata Santiago, Soo Kyung Kim, and Joanne Taery Kim. Deep symbolic regression: Recovering mathematical expressions from data via risk-seeking policy gradients. In *Proc. of ICLR*, 2021.
- Esteban Real, Alok Aggarwal, Yanping Huang, and Quoc V Le. Regularized evolution for image classifier architecture search. In *Proceedings of the aaai conference on artificial intelligence*, volume 33, pp. 4780–4789, 2019.
- Skipper Seabold and Josef Perktold. statsmodels: Econometric and statistical modeling with python. In *9th Python in Science Conference*, 2010.
- Yanne MG Soares and Roberta AA Fagundes. Interval quantile regression models based on swarm intelligence. *Applied Soft Computing*, 72:474–485, 2018.

- Ingo Steinwart and Andreas Christmann. Estimating conditional quantiles with the help of the pinball loss. *Bernoulli*, 17(1):211–225, 2011. ISSN 13507265.
- Robert L Thorndike. Who belongs in the family? *Psychometrika*, 18(4):267–276, 1953.
- Sergiy Verstyuk and Michael R Douglas. Machine learning the gravity equation for international trade. *SSRN*, 2022. doi: 10.2139/ssrn.4053795.
- Marco Virgolin, Ziyuan Wang, Tanja Alderliesten, and Peter AN Bosman. Machine learning for the prediction of pseudorealistic pediatric abdominal phantoms for radiation dose reconstruction. *Journal of Medical Imaging*, 7(4):046501–046501, 2020.
- Samantha Visbeek, Erman Acar, and Floris den Hengst. Explainable fraud detection with deep symbolic classification. In *World Conference on Explainable Artificial Intelligence*, pp. 350–373. Springer, 2024.
- Xiaohu Zheng, Jun Zhang, Guijian Tang, Tingsong Jiang, Wei Peng, and Wen Yao. A reliability analysis method based on quantile regression and feedforward neural network. In *12th International Conference on Quality, Reliability, Risk, Maintenance, and Safety Engineering*, volume 2022, pp. 294–300. IET, 2022.

## A Quantile Dependence of the Pinball Loss

To illustrate the potential quantile dependence of the pinball loss consider the following example:

For 100 predictions at the 50th quantile, one expects 50 predictions to be below the target and 50 above the target, resulting in a simplified mean pinball loss of:

$$\text{Mean Pinball Loss}_{50th} = \frac{(50 \times 0.5) + (50 \times 0.5)}{100} = 0.5$$

For 100 predictions at the 90th quantile, one expects 10 predictions to be below the target and 90 above the target, leading to:

$$\text{Mean Pinball Loss}_{90th} = \frac{(10 \times 0.9) + (90 \times 0.1)}{100} = 0.18$$

Although this calculation does not account for the extent to which the model overpredicts or underpredicts, it suggests that the pinball loss at the 90th quantile is generally lower than the pinball loss at the 50th quantile, irrespective of the predictive power. This hypothesis is further supported by the quantitative results presented in this thesis.

The asymmetrical nature of the pinball loss metric indicates its dependence on the chosen quantile, which poses challenges for consistent evaluation across different quantiles.

## B Model Parsimony Details

Table 5: Model Parsimony Weights

SQR Complexity	
Token	Complexity
$+$ , $-$ , $\times$ , Feature, Constant	1
$\div$ , square	2
$\sin$ , $\cos$	3
$\exp$ , $\log$ , $\sqrt{\cdot}$	4
LQR Complexity	
Feature, Bias	1
QDT Complexity	
Node	1

## C Statistical Testing

For the 50th quantile:

- **H0<sub>1,50</sub>**: SQR does not significantly outperform other quantile regressors in terms of Normalized Pinball Loss on the benchmark dataset.
- **H1<sub>1,50</sub>**: SQR significantly outperforms other quantile regressors in terms of Normalized Pinball Loss on the benchmark dataset.
- **H0<sub>2,50</sub>**: SQR does not significantly outperform other quantile regressors in terms of empirical coverage (Absolute Coverage Error) on the benchmark dataset.
- **H1<sub>2,50</sub>**: SQR significantly outperforms other quantile regressors in terms of empirical coverage (Absolute Coverage Error) on the benchmark dataset.
- **H0<sub>3,50</sub>**: SQR does not significantly outperform other quantile regressors in terms of Model parsimony on the benchmark dataset.
- **H1<sub>3,50</sub>**: SQR significantly outperforms other quantile regressors in terms of Model parsimony on the benchmark dataset.

For the 90th quantile:

- **H0<sub>1,90</sub>**: SQR does not significantly outperform other quantile regressors in terms of Normalized Pinball Loss on the benchmark dataset.
- **H1<sub>1,90</sub>**: SQR significantly outperforms other quantile regressors in terms of Normalized Pinball Loss on the benchmark dataset.

Table 6: Significance of results with Bonferroni-corrected Friedman tests.

Metric	Abbr.	$\tau$	Test statistic	p-value	significant
Normalized quantile loss	nql	0.5	311.63	$< 0.001$	<b>Yes</b>
Absolute coverage error	ace	0.5	18.67	$< 0.001$	<b>Yes</b>
Parsimony	c	0.5	516.76	$< 0.001$	<b>Yes</b>
Normalized quantile loss	nql	0.9	495.45	$< 0.001$	<b>Yes</b>
Absolute coverage error	ace	0.9	302.63	$< 0.001$	<b>Yes</b>
Parsimony	c	0.9	242.86	$< 0.001$	<b>Yes</b>

Table 7: Pairwise Wilcoxon Signed-Rank Test Results for  $\tau = 0.5$ .

Metric	Abbr.	Models	$T$ -statistic	p-value	Significant
Normalized quantile loss	nql	SQR vs QDT	35440.0	$< 0.001$	<b>Yes</b>
		SQR vs LQR	12151.0	$< 0.001$	<b>Yes</b>
		QDT vs LQR	21771.0	$< 0.001$	<b>Yes</b>
Absolute coverage error	ace	SQR vs QDT	67020.5	0.4670	No
		SQR vs LQR	53296.0	$< 0.001$	<b>Yes</b>
		QDT vs LQR	53257.0	$< 0.001$	<b>Yes</b>
Parsimony	pars	SQR vs QDT	3187.0	$< 0.001$	<b>Yes</b>
		SQR vs LQR	39726.0	$< 0.001$	<b>Yes</b>
		QDT vs LQR	9425.0	$< 0.001$	<b>Yes</b>

Table 8: Pairwise Wilcoxon Signed-Rank Test Results for  $\tau = .9$ .

Metric	Abbr.	Models	$T$ -statistic	p-value	Significant
Normalized quantile loss	nql	SQR vs QDT	30982.0	$< 0.001$	<b>Yes</b>
		SQR vs LQR	8134.0	$< 0.001$	<b>Yes</b>
		QDT vs LQR	8059.0	$< 0.001$	<b>Yes</b>
Absolute coverage error	ace	SQR vs QDT	39604.0	$< 0.001$	<b>Yes</b>
		SQR vs LQR	10842.5	$< 0.001$	<b>Yes</b>
		QDT vs LQR	14197.0	$< 0.001$	<b>Yes</b>
Parsimony	pars	SQR vs QDT	11966.0	$< 0.001$	<b>Yes</b>
		SQR vs LQR	39098.0	$< 0.001$	<b>Yes</b>
		QDT vs LQR	30847.5	$< 0.001$	<b>Yes</b>

- **H0<sub>2,90</sub>**: SQR does not significantly outperform other quantile regressors in terms of empirical coverage (Absolute Coverage Error) on the benchmark dataset.
- **H1<sub>2,90</sub>**: SQR significantly outperforms other quantile regressors in terms of empirical coverage (Absolute Coverage Error) on the benchmark dataset.
- **H0<sub>3,90</sub>**: SQR does not significantly outperform other quantile regressors in terms of Model parsimony on the benchmark dataset.
- **H1<sub>3,90</sub>**: SQR significantly outperforms other quantile regressors in terms of Model parsimony on the benchmark dataset.

## D Settings and hyperparameters

Table 9: PySRRegressor Parameters

Parameter	Value	Parameter	Value
maxsize	20	fraction_replaced	0.000364
maxdepth	None	fraction_replaced_hof	0.035
niterations	40	migration	True
populations	15	hof_migration	True
population_size	33	topn	12
ncycles_per_iteration	550	denoise	False
model_selection	'best'	select_k_features	None
dimensional_constraint_penalty	1000.0	max_evals	None
parsimony	0.0032	timeout_in_seconds	None
constraints	None	early_stop_condition	None
nested_constraints	None	procs	cpu_count()
complexity_of_operators	None	multithreading	True
complexity_of_constants	1	cluster_manager	None
complexity_of_variables	1	heap_size_hint_in_bytes	None
warmup_maxsize_by	0.0	batching	False
use_frequency	True	batch_size	50
use_frequency_in_tournament	True	precision	32
adaptive_parsimony_scaling	20.0	fast_cycle	False
should_simplify	True	turbo	False
weight_add_node	0.79	bumper	False
weight_insert_node	5.1	enable_autodiff	False
weight_delete_node	1.7	random_state	None
weight_do_nothing	0.21	deterministic	False
weight_mutate_constant	0.048	warm_start	False
weight_mutate_operator	0.47	verbosity	1
weight_swap_operands	0.1	update_verbosity	None
weight_randomize	0.00023	print_precision	5
weight_simplify	0.0020	progress	True
weight_optimize	0.0	temp_equation_file	False
crossover_probability	0.066	tempdir	None
annealing	False	delete_tempfiles	True
alpha	0.1	update	False
perturbation_factor	0.076	tournament_selection_n	10
skip_mutation_failures	True	tournament_selection_p	0.86
optimizer_algorithm	"BFGS"	optimizer_nrestarts	2
optimize_probability	0.14	optimizer_iterations	8
should_optimize_constants	True		



Table 10: Hyperparameters optimized through Optuna for each model in the quantitative evaluation

<b>LGBM</b>	
<b>Hyperparameter</b>	<b>Optimization Range</b>
num_leaves	2 to 100
learning_rate	0.01 to 0.5 (log-uniform)
max_depth	1 to 20
min_child_samples	5 to 100
<b>QDT</b>	
min_samples_leaf	1 to 50
<b>LQR</b>	
max_iter	1000 to 10000

## E Additional Results

Table 11: Extensive results overview

$\tau$	ID	$n$	$d$	Parsimony			Absolute Coverage Error				Quantile Loss				Time (ms)			
				QDT	LQR	SQR	QDT	LGBM	LQR	SQR	QDT	LGBM	LQR	SQR	QDT	LGBM	LQR	SQR
.5	1027	488	4	127.00	34.00	8.60	0.28	0.05	0.02	0.30	0.03	0.04	0.03	0.04	0.05	0.18	1.55	417.37
	1028	1000	10	101.40	31.00	3.00	0.27	0.07	0.03	0.21	0.07	0.08	0.08	0.08	0.06	0.30	1.81	607.82
	1029	1000	4	165.80	20.00	3.00	0.30	0.05	0.03	0.23	0.05	0.07	0.06	0.08	0.08	0.35	1.24	644.40
	1030	1000	4	42.20	4.00	3.20	0.11	0.06	0.05	0.05	0.08	0.08	0.08	0.08	0.04	0.28	0.09	630.11
	1089	47	13	7.00	14.00	11.20	0.16	0.10	0.14	0.14	0.06	0.12	0.06	0.06	0.02	0.02	1.94	278.11
	1096	50	4	11.40	5.00	14.40	0.14	0.08	0.06	0.16	0.04	0.08	0.01	0.01	0.02	0.02	0.09	285.53
	1193	31104	9	787.80	23.00	3.20	0.01	0.01	0.00	0.00	0.04	0.04	0.04	0.05	1.74	39.87	9.50	46954.57
	1199	17496	9	467.80	12.00	2.00	0.01	0.03	0.01	0.15	0.06	0.06	0.06	0.06	1.40	72.87	4.09	11112.44
	192	52	2	7.00	2.00	6.40	0.09	0.17	0.17	0.06	0.05	0.07	0.06	0.04	0.02	0.02	0.06	280.82
	197	8192	21	580.20	21.00	4.00	0.11	0.02	0.06	0.02	0.01	0.02	0.06	0.02	1.27	1.07	48.82	5003.10
	201	15000	48	1180.20	48.00	10.40	0.43	0.18	0.01	0.23	0.01	0.03	0.13	0.07	0.82	2.07	110.24	6569.89
	210	108	5	27.00	9.00	5.00	0.08	0.09	0.09	0.09	0.03	0.03	0.02	0.02	0.02	0.07	0.17	309.27
	215	40768	10	1013.80	29.00	14.20	0.00	0.00	0.00	0.00	0.02	0.02	0.04	0.03	1.52	222.50	18.67	62236.88
	218	22784	8	722.20	8.00	5.00	0.02	0.02	0.01	0.04	0.02	0.02	0.02	0.02	2.10	55.59	23.86	21459.98
	225	8192	8	252.60	8.00	3.00	0.01	0.01	0.10	0.16	0.05	0.05	0.08	0.06	0.90	38.36	1.32	10376.78
	227	8192	12	744.20	12.00	5.60	0.09	0.02	0.06	0.01	0.01	0.02	0.06	0.02	0.99	1.00	6.54	4147.02
	228	55	2	8.20	2.00	7.40	0.14	0.08	0.14	0.17	0.05	0.07	0.14	0.04	0.02	0.04	0.11	285.09
	229	200	10	63.40	29.00	9.20	0.06	0.06	0.08	0.11	0.04	0.04	0.04	0.05	0.02	0.10	0.85	331.74
	230	209	6	64.60	6.00	5.00	0.08	0.12	0.15	0.11	0.02	0.02	0.02	0.01	0.02	0.10	0.87	332.86
	294	6435	36	402.20	36.00	5.40	0.42	0.05	0.03	0.02	0.03	0.05	0.11	0.09	0.95	0.87	6.28	2485.58
	344	40768	10	12764.20	14.00	11.60	0.01	0.06	0.01	0.10	0.00	0.01	0.03	0.00	3.48	19.61	3.56	54050.23
	4544	1059	117	43.40	117.00	4.20	0.03	0.03	0.03	0.03	0.03	0.03	0.02	0.03	0.63	0.52	58.03	682.21
	485	48	4	11.80	12.00	18.80	0.06	0.17	0.12	0.21	0.06	0.11	0.06	0.05	0.02	0.02	0.04	263.80
	503	6574	14	241.40	14.00	2.00	0.02	0.01	0.01	0.01	0.03	0.03	0.03	0.04	0.94	0.98	2.24	2449.37
	505	240	124	66.60	124.00	12.60	0.08	0.03	0.06	0.04	0.01	0.02	0.00	0.01	0.09	0.16	212.41	403.18
	519	380	2	35.40	5.00	2.00	0.11	0.04	0.05	0.06	0.04	0.04	0.04	0.04	0.03	0.14	0.10	416.16
	522	500	7	48.20	7.00	6.20	0.04	0.05	0.06	0.04	0.06	0.06	0.07	0.07	0.04	0.19	0.09	475.29
	523	100	2	3.00	6.00	3.00	0.37	0.13	0.25	0.21	0.03	0.04	0.03	0.03	0.01	0.05	0.03	286.35
	527	67	14	18.20	14.00	15.20	0.17	0.11	0.50	0.50	0.02	0.04	0.00	0.00	0.02	0.05	0.02	257.00
	529	3848	4	477.40	4.00	4.00	0.03	0.02	0.01	0.01	0.03	0.03	0.02	0.03	0.36	0.88	0.22	1670.74
	537	20640	8	1590.20	8.00	2.00	0.38	0.38	0.40	0.43	0.04	0.06	0.06	0.08	NaN	NaN	NaN	NaN
	542	60	15	7.80	15.00	8.80	0.17	0.07	0.13	0.17	0.06	0.06	0.07	0.07	0.02	0.05	0.50	286.53
	547	500	7	32.20	7.00	3.00	0.03	0.04	0.05	0.05	0.04	0.04	0.04	0.05	0.06	0.22	0.30	445.13
	556	475	3	101.80	11.00	9.00	0.16	0.10	0.06	0.10	0.01	0.02	0.02	0.01	0.05	0.18	0.12	382.88
	557	475	3	83.40	11.00	3.80	0.19	0.13	0.06	0.10	0.01	0.02	0.02	0.01	0.04	0.18	0.16	379.58
	560	252	14	79.80	14.00	10.80	0.04	0.05	0.10	0.07	0.01	0.01	0.03	0.00	0.04	0.12	0.91	325.69
	561	209	7	52.20	7.00	10.60	0.11	0.13	0.05	0.05	0.01	0.01	0.01	0.00	0.03	0.10	0.17	325.50
	562	8192	12	744.20	12.00	5.60	0.09	0.02	0.06	0.01	0.01	0.02	0.06	0.02	1.20	0.99	6.76	4128.40
	564	40768	10	5656.60	10.00	10.60	0.01	0.01	0.01	0.01	0.02	0.03	0.03	0.02	3.60	22.54	6.24	54467.68
	573	8192	21	580.20	21.00	4.00	0.11	0.02	0.06	0.02	0.01	0.02	0.06	0.02	1.55	1.14	51.64	4988.03
	574	22784	16	921.80	16.00	3.40	0.03	0.03	0.00	0.00	0.02	0.02	0.02	0.03	3.68	65.43	31.43	28777.25
	579	250	5	61.00	5.00	14.00	0.03	0.05	0.05	0.03	0.06	0.05	0.05	0.03	0.03	0.13	0.13	369.25
	581	500	25	104.60	25.00	10.80	0.03	0.02	0.05	0.07	0.04	0.03	0.06	0.02	0.09	0.22	0.95	587.65
	582	500	25	119.00	25.00	11.20	0.06	0.04	0.02	0.08	0.04	0.04	0.08	0.03	0.10	0.24	1.67	589.31
	583	1000	50	122.60	50.00	13.60	0.02	0.03	0.03	0.04	0.04	0.03	0.08	0.02	0.35	0.42	31.36	844.05
	584	500	25	140.60	25.00	13.00	0.04	0.04	0.01	0.04	0.04	0.03	0.07	0.01	0.09	0.24	0.78	598.48
	588	1000	100	138.60	100.00	13.00	0.03	0.04	0.01	0.05	0.03	0.02	0.06	0.01	0.63	0.49	43.78	833.32
	589	1000	25	194.20	25.00	10.40	0.02	0.03	0.02	0.05	0.04	0.03	0.07	0.03	0.19	0.39	1.56	954.59
	590	1000	50	104.60	50.00	13.80	0.04	0.04	0.04	0.05	0.05	0.04	0.04	0.02	0.34	0.44	79.81	742.22
	591	100	10	13.00	10.00	16.60	0.07	0.07	0.05	0.15	0.06	0.07	0.09	0.01	0.02	0.07	0.79	314.17
592	1000	25	251.40	25.00	11.60	0.06	0.05	0.05	0.03	0.03	0.03	0.06	0.02	0.24	0.40	1.53	946.77	
593	1000	10	250.20	10.00	13.80	0.04	0.04	0.03	0.07	0.03	0.03	0.07	0.02	0.10	0.35	0.20	817.72	
594	100	5	17.00	5.00	12.80	0.16	0.13	0.17	0.12	0.06	0.07	0.09	0.04	0.02	0.07	0.16	314.67	
595	1000	10	101.00	10.00	14.00	0.02	0.03	0.05	0.02	0.04	0.03	0.04	0.02	0.12	0.37	0.27	680.13	
596	250	5	47.40	5.00	13.80	0.05	0.08	0.06	0.02	0.05	0.05	0.09	0.02	0.03	0.13	0.16	386.82	
597	500	5	107.80	5.00	14.40	0.06	0.06	0.04	0.04	0.04	0.04	0.08	0.02	0.06	0.21	0.16	504.96	
598	1000	25	108.60	25.00	14.20	0.04	0.02	0.03	0.04	0.05	0.04	0.04	0.02	0.26	0.40	1.08	885.33	
599	1000	5	329.40	5.00	11.40	0.04	0.03	0.03	0.04	0.03	0.03	0.08	0.02	0.10	0.33	0.28	768.03	
601	250	5	79.40	5.00	13.80	0.06	0.06	0.04	0.08	0.04	0.04	0.07	0.02	0.03	0.12	0.12	395.85	
602	250	10	63.00	10.00	9.80	0.06	0.08	0.09	0.04	0.04	0.04	0.07	0.02	0.03	0.13	0.16	378.80	
603	250	50	16.20	50.00	10.60	0.05	0.09	0.06	0.12	0.05	0.04	0.04	0.02	0.06	0.15	60.95	400.30	
604	500	10	122.60	10.00	11.80	0.04	0.06	0.06	0.05	0.03	0.03							

$\tau$	ID	$n$	$d$	Parsimony			Absolute Coverage Error				Quantile Loss				Time (ms)			
				QDT	LQR	SQR	QDT	LGBM	LQR	SQR	QDT	LGBM	LQR	SQR	QDT	LGBM	LQR	SQR
	615	250	10	80.60	10.00	10.80	0.06	0.06	0.07	0.05	0.04	0.04	0.06	0.02	0.03	0.13	0.17	378.79
	616	500	50	107.80	50.00	13.20	0.06	0.06	0.03	0.05	0.04	0.03	0.07	0.02	0.16	0.27	26.79	565.06
	617	500	5	143.80	5.00	13.20	0.04	0.05	0.02	0.07	0.03	0.03	0.06	0.01	0.07	0.22	0.20	505.50
	618	1000	50	105.80	50.00	13.40	0.02	0.03	0.03	0.05	0.03	0.03	0.06	0.02	0.41	0.42	59.76	855.20
	620	1000	25	102.20	25.00	12.80	0.03	0.03	0.02	0.02	0.04	0.03	0.07	0.02	0.21	0.40	1.23	952.61
	621	100	10	15.40	10.00	12.60	0.09	0.08	0.07	0.05	0.06	0.06	0.05	0.03	0.02	0.07	0.09	305.17
	622	1000	50	120.60	50.00	13.00	0.04	0.02	0.02	0.06	0.04	0.03	0.08	0.03	0.31	0.42	68.44	872.94
	623	1000	10	287.00	10.00	11.20	0.02	0.02	0.03	0.10	0.02	0.02	0.05	0.02	0.18	0.39	0.53	808.82
	624	100	5	15.80	5.00	13.80	0.09	0.14	0.13	0.12	0.05	0.06	0.04	0.03	0.02	0.06	0.27	311.88
	626	500	50	69.80	50.00	12.40	0.06	0.05	0.03	0.05	0.04	0.04	0.08	0.02	0.17	0.27	24.94	570.77
	627	500	10	125.00	10.00	14.20	0.05	0.06	0.03	0.05	0.04	0.03	0.07	0.02	0.06	0.22	0.17	488.32
	628	1000	5	320.60	5.00	13.00	0.04	0.03	0.03	0.08	0.03	0.02	0.06	0.02	0.10	0.35	0.19	766.35
	631	500	5	125.00	5.00	14.80	0.05	0.02	0.02	0.02	0.04	0.04	0.07	0.02	0.05	0.20	0.88	490.51
	633	500	25	41.80	25.00	12.40	0.03	0.02	0.06	0.04	0.05	0.04	0.04	0.03	0.10	0.23	1.91	536.16
	634	100	10	17.80	10.00	10.80	0.09	0.09	0.09	0.08	0.06	0.07	0.08	0.05	0.02	0.07	0.92	309.55
	635	250	10	31.40	10.00	11.60	0.05	0.04	0.05	0.06	0.05	0.05	0.05	0.03	0.04	0.13	0.25	359.96
	637	500	50	79.80	50.00	12.40	0.04	0.05	0.04	0.03	0.04	0.04	0.08	0.02	0.15	0.27	28.30	567.91
	641	500	10	161.80	10.00	14.80	0.03	0.03	0.06	0.07	0.04	0.04	0.08	0.01	0.08	0.23	0.48	495.00
	643	500	25	75.80	25.00	11.80	0.05	0.03	0.05	0.03	0.04	0.04	0.08	0.02	0.11	0.24	0.61	610.85
	644	250	25	54.20	25.00	12.40	0.04	0.05	0.03	0.05	0.04	0.04	0.08	0.02	0.04	0.13	0.60	417.86
	645	500	50	86.20	50.00	12.00	0.03	0.07	0.06	0.05	0.03	0.03	0.06	0.02	0.19	0.25	12.81	558.50
	646	500	10	161.40	10.00	13.20	0.06	0.05	0.03	0.05	0.03	0.03	0.06	0.01	0.09	0.24	0.66	494.46
	647	250	10	37.80	10.00	14.00	0.04	0.06	0.04	0.03	0.04	0.04	0.08	0.02	0.04	0.14	0.37	393.58
	648	250	50	53.40	50.00	13.40	0.05	0.04	0.08	0.05	0.05	0.04	0.09	0.02	0.08	0.15	8.67	424.57
	649	500	5	141.80	5.00	13.60	0.03	0.07	0.05	0.07	0.04	0.03	0.03	0.02	0.05	0.19	0.21	435.42
	650	500	50	46.60	50.00	13.80	0.04	0.02	0.05	0.04	0.05	0.04	0.04	0.02	0.13	0.25	58.40	513.67
	651	100	25	8.60	25.00	10.80	0.06	0.13	0.11	0.13	0.07	0.08	0.06	0.03	0.02	0.08	0.71	319.38
	653	250	25	23.80	25.00	12.20	0.06	0.05	0.08	0.10	0.05	0.05	0.04	0.02	0.04	0.14	0.95	389.50
	654	500	10	69.40	10.00	12.00	0.03	0.06	0.04	0.04	0.04	0.04	0.04	0.03	0.06	0.23	0.16	437.26
	656	100	5	25.00	5.00	11.40	0.11	0.17	0.10	0.12	0.06	0.07	0.09	0.03	0.02	0.07	0.38	316.60
	657	250	10	59.00	10.00	11.20	0.07	0.03	0.08	0.06	0.05	0.05	0.08	0.03	0.04	0.14	0.33	378.94
	658	250	25	43.80	25.00	11.80	0.04	0.04	0.04	0.06	0.04	0.04	0.06	0.02	0.04	0.15	1.29	411.38
	659	47	7	9.80	7.00	11.20	0.20	0.16	0.14	0.16	0.04	0.06	0.04	0.04	0.02	0.02	0.44	280.43
	663	120	2	18.60	11.00	14.80	0.12	0.09	0.06	0.07	0.04	0.04	0.01	0.01	0.02	0.07	0.11	314.80
	665	147	6	13.40	10.00	2.40	0.19	0.12	0.08	0.07	0.05	0.06	0.06	0.06	0.02	0.09	0.70	309.44
	666	508	10	29.00	10.00	2.40	0.06	0.05	0.04	0.04	0.03	0.03	0.03	0.03	0.05	0.20	0.49	469.00
	678	111	3	5.80	3.00	4.40	0.23	0.20	0.10	0.19	0.06	0.07	0.07	0.07	0.02	0.07	0.07	330.22
	687	62	5	10.60	5.00	6.80	0.10	0.07	0.13	0.05	0.06	0.08	0.06	0.07	0.02	0.05	0.09	291.70
	690	323	4	91.40	10.00	7.40	0.07	0.05	0.03	0.06	0.02	0.02	0.03	0.02	0.05	0.15	0.35	351.65
	695	235	12	11.40	12.00	6.80	0.06	0.07	0.05	0.06	0.03	0.03	0.02	0.02	0.03	0.11	0.29	364.61
	706	93	6	9.00	11.00	5.20	0.12	0.17	0.05	0.06	0.05	0.06	0.05	0.05	0.02	0.05	1.01	303.72
	712	222	2	11.80	2.00	3.40	0.11	0.12	0.09	0.12	0.05	0.05	0.09	0.05	0.02	0.10	0.09	385.31
	banana	5300	2	197.40	2.00	8.40	0.44	0.05	0.23	0.05	0.05	0.09	0.22	0.08	0.23	0.80	0.04	4244.90
	titanic	2099	8	143.00	31.00	5.20	0.35	0.18	0.15	0.34	0.10	0.11	0.11	0.10	0.17	0.57	0.83	859.30
.9	1027	488	4	127.00	34.00	9.00	0.02	0.02	0.09	0.06	0.01	0.02	0.01	0.02	0.05	0.15	0.83	417.99
	1028	1000	10	65.40	31.00	3.00	0.07	0.10	0.04	0.09	0.03	0.04	0.03	0.03	0.06	0.05	2.02	632.44
	1029	1000	4	49.80	20.00	4.60	0.07	0.01	0.03	0.06	0.03	0.03	0.03	0.03	0.06	0.30	1.06	670.53
	1030	1000	4	34.60	4.00	4.20	0.04	0.03	0.05	0.04	0.03	0.04	0.04	0.04	0.05	0.28	0.21	601.44
	1089	47	13	7.00	14.00	9.40	0.14	0.07	0.23	0.15	0.02	0.05	0.06	0.02	0.02	0.03	0.61	278.51
	1096	50	4	8.60	5.00	13.20	0.18	0.04	0.16	0.06	0.02	0.05	0.00	0.00	0.02	0.03	0.06	272.76
	1193	31104	9	821.80	23.00	3.00	0.02	0.02	0.00	0.00	0.02	0.02	0.02	0.02	1.96	68.27	18.54	17203.20
	1199	17496	9	457.00	12.00	3.60	0.03	0.01	0.00	0.00	0.03	0.03	0.03	0.03	1.30	123.39	3.98	6687.39
	192	52	2	5.00	2.00	8.80	0.08	0.10	0.10	0.19	0.02	0.03	0.03	0.06	0.02	0.03	0.09	279.64
	197	8192	21	250.20	21.00	6.20	0.01	0.02	0.03	0.01	0.00	0.01	0.03	0.01	1.36	0.98	48.52	3736.67
	201	15000	48	619.80	48.00	11.40	0.07	0.10	0.01	0.02	0.01	0.07	0.05	0.04	1.28	0.19	104.02	5202.34
	210	108	5	11.00	9.00	7.40	0.08	0.07	0.08	0.05	0.02	0.02	0.01	0.01	0.02	0.08	0.19	300.22
	215	40768	10	997.80	29.00	12.80	0.02	0.05	0.00	0.01	0.01	0.01	0.02	0.01	2.01	453.39	15.57	35646.02
	218	22784	8	613.00	8.00	7.40	0.03	0.03	0.00	0.01	0.01	0.01	0.02	0.01	2.09	59.85	109.11	8624.05
	225	8192	8	210.20	8.00	4.20	0.02	0.01	0.50	0.01	0.02	0.02	0.09	0.02	0.70	66.04	1.36	6343.11
	227	8192	12	247.80	12.00	4.80	0.01	0.01	0.03	0.01	0.00	0.01	0.03	0.01	1.29	0.92	15.89	4341.78
	228	55	2	10.20	2.00	6.40	0.06	0.07	0.09	0.07	0.02							

$\tau$	ID	$n$	$d$	Parsimony			Absolute Coverage Error				Quantile Loss				Time (ms)			
				QDT	LQR	SQR	QDT	LGBM	LQR	SQR	QDT	LGBM	LQR	SQR	QDT	LGBM	LQR	SQR
542	60	15		5.40	15.00	8.40	0.06	0.05	0.15	0.14	0.03	0.03	0.05	0.04	0.02	0.06	1.83	280.26
547	500	7		31.80	7.00	5.80	0.04	0.02	0.05	0.03	0.02	0.02	0.02	0.02	0.06	0.19	0.30	451.30
556	475	3		87.80	11.00	6.80	0.06	0.03	0.04	0.17	0.00	0.02	0.02	0.01	0.04	0.16	1.33	384.64
557	475	3		83.00	11.00	7.00	0.04	0.03	0.04	0.14	0.00	0.02	0.02	0.01	0.06	0.17	1.18	377.32
560	252	14		70.60	14.00	13.60	0.19	0.06	0.04	0.04	0.00	0.02	0.02	0.00	0.04	0.09	0.77	326.68
561	209	7		58.60	7.00	10.00	0.09	0.06	0.03	0.04	0.01	0.01	0.01	0.00	0.03	0.08	0.94	328.90
562	8192	12		247.80	12.00	4.80	0.01	0.01	0.03	0.01	0.00	0.01	0.03	0.01	1.18	0.90	16.45	4347.84
564	40768	10		2332.60	10.00	11.40	0.06	0.03	0.01	0.00	0.01	0.01	0.01	0.01	4.29	207.23	10.34	25297.07
574	22784	16		677.40	16.00	6.40	0.03	0.03	0.00	0.01	0.01	0.01	0.02	0.02	3.71	65.68	34.81	10718.79
579	250	5		22.60	5.00	10.00	0.07	0.02	0.46	0.04	0.03	0.03	0.05	0.01	0.03	0.11	0.14	348.76
581	500	25		57.00	25.00	14.20	0.11	0.03	0.46	0.04	0.02	0.02	0.07	0.01	0.09	0.18	1.46	577.45
582	500	25		43.40	25.00	13.00	0.06	0.02	0.43	0.03	0.02	0.02	0.08	0.01	0.13	0.21	1.62	567.63
583	1000	50		53.00	50.00	13.00	0.05	0.02	0.43	0.02	0.02	0.02	0.08	0.01	0.34	0.34	56.88	840.03
584	500	25		42.60	25.00	11.20	0.11	0.04	0.43	0.02	0.02	0.02	0.07	0.01	0.11	0.19	2.91	614.10
586	1000	25		89.40	25.00	14.00	0.09	0.02	0.42	0.01	0.01	0.02	0.06	0.01	0.19	0.29	0.96	938.14
588	1000	100		55.80	100.00	12.20	0.06	0.01	0.45	0.02	0.01	0.02	0.07	0.01	0.69	0.36	92.25	807.68
589	1000	25		61.80	25.00	12.00	0.06	0.02	0.43	0.02	0.02	0.02	0.07	0.01	0.18	0.32	1.08	1058.47
590	1000	50		36.20	50.00	11.00	0.05	0.02	0.47	0.02	0.02	0.02	0.04	0.01	0.33	0.34	82.32	663.92
591	100	10		8.60	10.00	12.00	0.08	0.09	0.40	0.07	0.03	0.03	0.10	0.01	0.03	0.08	0.41	312.11
592	1000	25		52.20	25.00	11.20	0.06	0.03	0.44	0.02	0.02	0.02	0.06	0.01	0.22	0.29	1.74	928.71
593	1000	10		61.00	10.00	13.80	0.07	0.01	0.44	0.02	0.02	0.02	0.07	0.01	0.15	0.30	0.35	827.27
594	100	5		9.00	5.00	13.80	0.04	0.04	0.49	0.04	0.02	0.03	0.11	0.01	0.02	0.08	0.28	319.98
595	1000	10		38.60	10.00	10.00	0.06	0.03	0.41	0.01	0.02	0.02	0.04	0.01	0.15	0.31	0.39	624.37
596	250	5		15.40	5.00	12.40	0.09	0.05	0.40	0.07	0.03	0.03	0.09	0.01	0.03	0.13	0.10	404.04
597	500	5		32.60	5.00	12.20	0.05	0.02	0.42	0.03	0.02	0.02	0.08	0.01	0.05	0.19	0.25	521.49
598	1000	25		45.80	25.00	12.60	0.04	0.01	0.43	0.03	0.02	0.02	0.05	0.01	0.20	0.31	0.79	761.18
599	1000	5		77.80	5.00	13.80	0.08	0.02	0.44	0.02	0.02	0.02	0.08	0.01	0.11	0.30	0.20	789.88
601	250	5		16.60	5.00	13.40	0.04	0.04	0.44	0.05	0.02	0.03	0.08	0.01	0.03	0.12	0.13	398.24
602	250	10		39.00	10.00	9.60	0.15	0.04	0.50	0.03	0.02	0.02	0.07	0.01	0.04	0.13	0.39	368.25
603	250	50		12.60	50.00	11.40	0.04	0.04	0.46	0.04	0.02	0.02	0.05	0.01	0.05	0.13	45.19	367.35
604	500	10		67.80	10.00	12.40	0.10	0.04	0.46	0.01	0.02	0.02	0.06	0.01	0.07	0.19	0.80	459.87
605	250	25		10.60	25.00	12.20	0.03	0.03	0.43	0.05	0.02	0.03	0.09	0.01	0.04	0.13	0.97	432.07
606	1000	10		43.40	10.00	10.00	0.05	0.03	0.43	0.02	0.02	0.02	0.07	0.01	0.16	0.32	0.73	875.80
607	1000	50		71.40	50.00	13.40	0.08	0.02	0.42	0.02	0.01	0.01	0.06	0.01	0.39	0.33	27.36	829.80
608	1000	10		53.00	10.00	12.60	0.05	0.02	0.44	0.01	0.01	0.01	0.06	0.01	0.13	0.27	0.71	767.77
609	1000	5		55.80	5.00	9.60	0.05	0.03	0.40	0.03	0.02	0.02	0.04	0.01	0.12	0.30	0.34	589.04
611	100	5		11.40	5.00	12.00	0.08	0.13	0.44	0.08	0.03	0.03	0.09	0.01	0.02	0.07	0.18	307.26
612	1000	5		96.60	5.00	13.60	0.08	0.01	0.43	0.02	0.02	0.02	0.07	0.01	0.11	0.28	0.36	786.96
613	250	5		34.20	5.00	11.80	0.09	0.04	0.42	0.03	0.02	0.02	0.07	0.01	0.03	0.13	0.13	387.20
615	250	10		23.00	10.00	12.60	0.07	0.06	0.44	0.06	0.02	0.02	0.06	0.01	0.03	0.12	0.36	352.36
616	500	50		37.00	50.00	12.40	0.08	0.03	0.44	0.03	0.02	0.02	0.08	0.01	0.17	0.21	51.08	551.43
617	500	5		71.40	5.00	9.60	0.09	0.02	0.41	0.04	0.01	0.02	0.06	0.01	0.05	0.17	0.41	480.17
618	1000	50		46.20	50.00	12.20	0.03	0.02	0.44	0.03	0.01	0.02	0.07	0.01	0.45	0.31	46.20	792.32
620	1000	25		28.20	25.00	12.60	0.03	0.03	0.43	0.02	0.02	0.02	0.07	0.01	0.20	0.32	1.44	955.78
621	100	10		7.40	10.00	11.60	0.05	0.02	0.46	0.08	0.03	0.03	0.05	0.01	0.02	0.08	0.21	287.23
622	1000	50		43.40	50.00	13.40	0.03	0.03	0.43	0.02	0.02	0.02	0.08	0.01	0.45	0.37	37.83	931.59
623	1000	10		57.40	10.00	13.20	0.05	0.02	0.42	0.02	0.01	0.01	0.05	0.01	0.16	0.29	0.64	783.34
624	100	5		8.60	5.00	10.80	0.07	0.07	0.48	0.13	0.03	0.03	0.05	0.02	0.02	0.08	0.27	289.30
626	500	50		40.20	50.00	14.60	0.09	0.05	0.44	0.04	0.02	0.02	0.09	0.01	0.17	0.22	18.70	616.20
627	500	10		33.00	10.00	13.40	0.06	0.03	0.43	0.03	0.02	0.02	0.07	0.01	0.06	0.20	0.33	513.07
628	1000	5		127.00	5.00	9.40	0.09	0.01	0.43	0.02	0.01	0.02	0.06	0.01	0.13	0.27	0.33	743.16
631	500	5		28.60	5.00	14.60	0.05	0.03	0.39	0.03	0.02	0.02	0.07	0.01	0.05	0.17	0.17	501.60
633	500	25		24.60	25.00	11.20	0.06	0.03	0.47	0.03	0.02	0.02	0.04	0.01	0.09	0.20	1.56	515.20
634	100	10		15.40	10.00	11.40	0.07	0.02	0.45	0.11	0.03	0.03	0.09	0.02	0.02	0.07	0.27	322.81
635	250	10		15.80	10.00	10.80	0.04	0.03	0.48	0.06	0.02	0.02	0.05	0.01	0.04	0.12	0.29	339.19
637	500	50		26.60	50.00	12.20	0.05	0.04	0.45	0.04	0.02	0.02	0.09	0.01	0.14	0.24	54.62	576.31
641	500	10		51.00	10.00	14.00	0.07	0.03	0.45	0.03	0.02	0.02	0.08	0.01	0.06	0.19	0.55	473.30
643	500	25		30.20	25.00	13.40	0.04	0.04	0.45	0.04	0.02	0.02	0.08	0.01	0.11	0.20	1.60	647.74
644	250	25		14.20	25.00	10.20	0.04	0.04	0.42	0.04	0.02	0.02	0.08	0.01	0.05	0.13	1.41	419.07
645	500	50		41.80	50.00	15.00	0.09	0.03	0.48	0.03	0.02	0.02	0.06	0.01	0.14	0.21	10.35	529.98
646	500	10		38.60	10.00	12.80	0.08	0.03	0.42	0.02	0.02	0.02	0.06	0.01	0.06	0.17	0.29	461.38
647	250	10		21.40	10.00	14.00	0.06	0.02	0.44	0.03	0.02	0.02	0.08	0.01	0.04	0.13	0.84	381.77
648	250	50		13.40	50.00	12.00	0.06	0.06	0.50	0.08	0.02	0.03	0.11	0.01	0.05	0.14	49.37	424.64
649	500	5		43.00	5.00	10.40	0.06	0.04	0.43	0.04	0.02	0.02	0.03	0.01	0.06	0.17	0.47	405.27
650	500	50		21.00	50.00	11.00	0.05	0.02	0.46	0.02	0.02	0.02	0.05	0.01	0.15	0.22	17.77	466.25
651	100	25		3.80	25.00	10.00	0.04	0.05	0.51	0.07	0.03	0.03	0.09	0.01	0.02	0.08	1.54	297.21
653	250	25		13.40	25.00	11.40	0.05	0.02	0.48	0.04	0.02	0.03	0.05	0.01	0.05	0.13	1.21	362.26
654	500	10		17.80	10.00	11.00	0.04	0.03	0.43	0.03	0.02	0.02	0.04	0.01	0.05	0.18	0.25	396.92
656	100	5		13.00	5.00	11.60	0.08	0.04	0.47	0.10	0.02	0.03	0.09	0.01	0.02	0.08	0.26	325.08
657	250	10		32.20	10.00	14.60	0.08	0										

$\tau$	ID	$n$	$d$	Parsimony			Absolute Coverage Error				Quantile Loss				Time (ms)			
				QDT	LQR	SQR	QDT	LGBM	LQR	SQR	QDT	LGBM	LQR	SQR	QDT	LGBM	LQR	SQR
	687	62	5	5.80	5.00	7.00	0.10	0.06	0.04	0.17	0.03	0.03	0.03	0.04	0.02	0.06	0.15	282.65
	690	323	4	59.80	10.00	7.00	0.07	0.03	0.04	0.03	0.01	0.02	0.01	0.01	0.04	0.12	0.45	357.64
	695	235	12	14.20	12.00	2.00	0.07	0.03	0.05	0.04	0.01	0.02	0.01	0.01	0.03	0.11	0.19	359.22
	706	93	6	5.40	11.00	8.60	0.04	0.02	0.09	0.09	0.03	0.03	0.02	0.02	0.02	0.07	0.85	300.67
	712	222	2	24.60	2.00	3.20	0.04	0.08	0.11	0.05	0.02	0.02	0.06	0.02	0.03	0.12	0.06	376.74
	banana	5300	2	146.60	2.00	12.60	0.09	0.10	0.64	0.35	0.03	0.06	0.40	0.04	0.20	0.13	0.05	2141.00
	titanic	2099	8	87.40	31.00	3.20	0.07	0.10	0.12	0.10	0.07	0.07	0.07	0.07	0.13	0.11	1.01	903.90

## F Reproducibility

All experiments were conducted on a local machine with the following specifications:

- **Operating System:** Microsoft Windows 10 Enterprise
- **Programming Language:** Python (with PySR using a Julia backbone)
- **Libraries and Frameworks:**
  - PySR
  - LGBM
  - scikit-learn
  - LogisticRegression (from sklearn.linear\_model)
  - KFold (from sklearn.model\_selection)
  - NumPy
  - Matplotlib
  - Seaborn
  - pandas
  - pmlb (Python Package for accessing PMLB datasets)
  - optuna
  - datetime (from Python standard library)